2.2. Fischer-Tropsch Product Distribution

In the last report, we evaluated the hydrocarbon product concentration profile in the catalyst pores in the presence of vapor liquid separation. It was shown theoretically that for light hydrocarbons (C_{20-}), the internal diffusion limitation decreases with increasing carbon number. It was argued that the diffusion model, which attributes the two alpha product distribution to the increased internal diffusion limitation with increasing carbon number, was not valid. The major assumption of the work in the last quarterly report was that all of the products are non-reactive paraffins. In practice, olefins are also produced and these have been confirmed experimentally to be reactive. In other words, the pathway for termination to olefins is reversible. This supplement to last quarter's report present the hydrocarbon concentration profile in the catalyst pores when olefin reincorporation is also taken into account.

Additional assumptions are required since little quantitative data are available for olefin reactions under Fischer-Tropsch synthesis conditions. As usual, it is assumed that chain growth on the catalyst surface follows a single α rule. For each chain growth intermediate, same olefin fraction is generated in the total hydrocarbons of that carbon number before considering the reversible reaction of olefins. For simplicity of discussion, it is further assumed that all of the products are olefins. The olefin reaction kinetics to higher hydrocarbons follows k_rC_i, in which k_r is the rate constant independent of carbon number. Finally, it is also assumed that the primary reaction of CO and H_2 are not affected by the olefin reaction.

Any hydrocarbon component i is generated from CO and H_2, from lighter olefins ranging from carbon 2 to carbon i-1, and is decreased by conversion to higher hydrocarbons at a rate of k_rC_i. The material balance of component i in the catalyst pores is shown in Equation (1).

$$D_i \frac{1}{r^2}\frac{d}{dr}\left(r^2 \frac{dC_i}{dr}\right) = -k_i C_H - \sum_{j=2}^{i-1} k_r (1-\alpha)\alpha^{i-j-1} C_j + k_r C_i \qquad (1)$$

The analytical solution to Equation (1) is

$$\frac{C_i}{C_{i,s}} = \left(1 - \sum_{j=1}^{i-1} B_{ij}\right)\left(\frac{R_p}{r}\right)\frac{\sinh(\phi_{ir} r / R_p)}{\sinh(\phi_{ir})} + \sum_{j=1}^{i-1} B_{ij}\left(\frac{C_j}{C_{j,s}}\right) \qquad (2)$$

In Equation (2), C_i and $C_{i,s}$ are the pore concentration and surface concentration of component i, respectively. R_p is the characteristic length of a catalyst pellet. Other parameters are defined in the following equations

$$B_{ij} = \frac{1-\alpha}{\alpha}\frac{\phi_{jr}^2}{\phi_{ir}^2 - \phi_{jr}^2}\left(\frac{\phi_i^2}{\phi_j^2} - \sum_{k=j+1}^{i-1} B_{ik}\frac{\phi_k^2}{\phi_j^2}\right) \qquad B_{i1} = \frac{\phi_H^2}{\phi_{ir}^2 - \phi_H^2}\left(\frac{\phi_i^2}{\phi_H^2} - \sum_{j=2}^{i-1} B_{ij}\frac{\phi_j^2}{\phi_H^2}\right)$$

$$\phi_H = R_p\sqrt{\frac{k_H}{D_H}} \qquad \phi_{ir} = R_p\sqrt{\frac{k_{ir}}{D_i}} \qquad \phi_i = R_p\sqrt{\frac{k_i}{D_i}\frac{C_{H,s}}{C_{i,s}}}$$

The reaction conditions used to illustrate the product concentration profile in the catalyst pores are 230 ºC, 40% CO conversion, α=0.85, Thiele modulus of H_2 = 2.0, and k_r/k_H = 0.025. The latter corresponds to about 10% of the olefins generated in the primary termination step being reincorporated into growing chains. Figure 1 shows the dependence of the volumetrically average concentration of product in the catalyst pores on the carbon number. When considering the reversible olefin reaction, the relative concentration of light products decreases even more rapidly than the situation of non-reactive paraffin products. It is clear that, with or without

considering olefin reaction, the relative concentration of light hydrocarbons (C_{20-}) decreases with increasing carbon number. This indicates that the chance of internal diffusion limitation decreases with increasing carbon number and should not be responsible for the two alpha product distribution in Fischer-Tropsch synthesis.

Task 3. Catalyst Characterization

The objective of this task is to obtain characterization data of the prepared catalysts using routine and selected techniques.

3.1. Mössbauer study of precipitated unpromoted and potassium promoted iron Fischer-Tropsch synthesis catalyst

Introduction

As the alternative route to synthesize hydrocarbons other than petroleum industry, Fischer-Tropsch synthesis has been one of the most extensively studied subject in catalysis for several decades. Although most of the recent effort in industry concentrated on cobalt catalyst, iron is still a promising catalyst due to its several advantages, especially for slurry phase reactor. The complexity of phase transformation of iron catalyst during activation and synthesis cause difficulty to accurately elucidate the active phase. Studies to correlate the structure of catalysts with FTS activity were conducted by different authors to define the active phase of iron catalyst. At present the question remains whether magnetite is active for FTS. Early work by Reymond et al (1) and recent work by Kuivila et al. (2) suggest that magnetite is the active phase. Reymond's experiments were performed on both unreduced and reduced iron catalyst. Similar hydrocarbon product distributions were found on these two catalysts, with a maximum activity occurring over a material consisting of approximately equal amounts of magnetite and Hägg carbide. Further carbide formation in the unreduced catalyst coincided with a diminished rate of FT synthesis;

therefore, it was concluded that magnetite is an active catalyst. Kuivila studied the reduced and unreduced iron catalyst using the combination of XPS and FTS performance. Their conclusion was based on the fact that they observed only magnetite on the surface of the catalyst after reaction. A similar study was carried out by Dictor and Bell (3) in a slurry-phase reactor using reduced and unreduced Fe_2O_3 powder. However, they concluded that the active phase is Hägg carbide and magnetite is not active.

The work described in this report shows that with appropriate methods to withdraw catalyst samples for characterization, the catalyst situation in the continuous stirred tank reactor can be revealed during activation and synthesis. Correlation between catalyst composition and FTS activity is made to define the nature of active phase. Comparison with results previously obtained on ultrafine iron catalyst and unpromoted precipitated iron catalyst is made in this report.

Experimental

Catalyst activation and FTS reaction

The catalyst used was prepared by continuous precipitation at a pH of about 9 from aqueous solution of $Fe(NO_3)_3 9H_2O$ and concentrated NH_4OH. The precipitate was throughly washed with distilled-deionized water and dried at 120^0C. A mixture of 64.44g iron catalyst which contains 50.00% Fe, 0.457g of $(CH_3)_3COK$ and 290g C_{30} startup oil (Shell decene trimer) was charged into a 1L autoclave operated as a continuous stirred tank reactor (CSTR). The catalyst slurry was heated to 270^0C at 2^0C/min under a flow rate of 2.0[NL/hg-(Fe)] CO. CO activation continued at 270^0C and 1.20MPa for 24h. Flowing activation, hydrogen flow was started to give a H_2/CO ratio of 0.68 with a flow rate of 3.1NL/hg-(Fe). Catalyst slurry samples (5-10g) were removed from the reactor under the protection of Ar following activation and

during different stages of synthesis. Mössbauer samples were prepared in sample holders in a glove bag filled with Ar. Wax products on the catalyst was extracted using THF as the solvent.

Mössbauer analysis

Mössbauer samples were loaded into plexiglass compression holders after extract of wax with THF in a glove bag filled with Ar.

Results

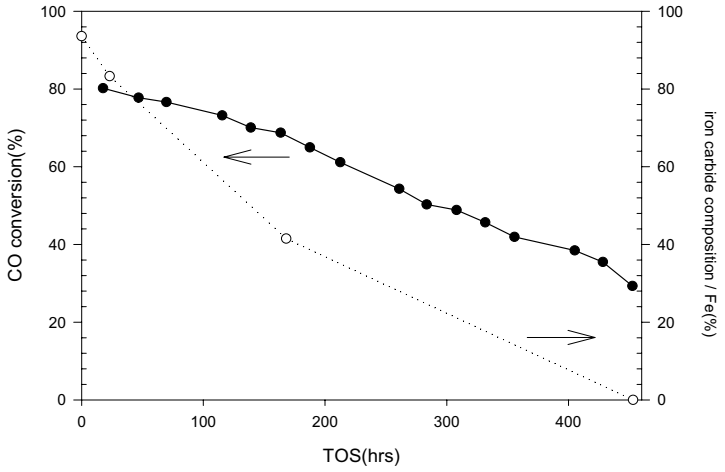

Fig. 1 Catalytic activity and iron carbide percentage versus reaction time

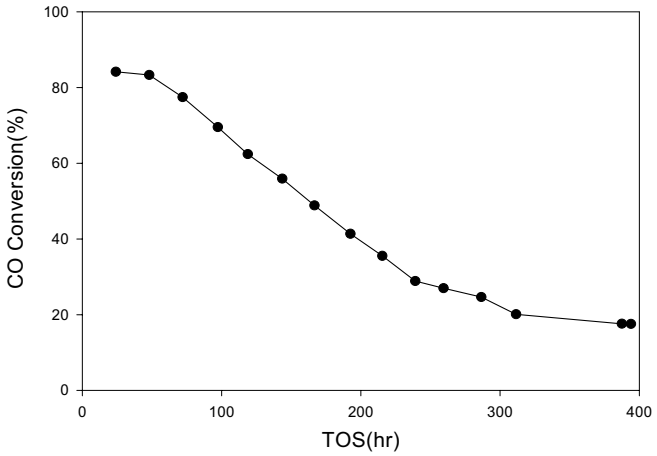

Fig 2. CO Conversion as a function of time on stream

Table 1

Mössbauer parameters for precipitated iron catalyst after activation and during synthesis

Sample	Site	HMF(KG)	IS(mm/s)	QS(mm/s)	FW(mm/s)	Fraction
After activation	Fe_3O_4 A	483	0.28	0.04	0.26	1.7
	Fe_3O_4 B	455	0.64	-0.08	0.41	4.4
	Fe_5C_2 I	220	0.26	0.04	0.40	33.6
	Fe_5C_2 II	182	0.20	-0.01	0.42	29.3
	Fe_5C_2 III	101	0.22	0.08	0.50	30.7
FTS run 23h	Fe_3O_4 A	485	0.32	-0.07	0.26	4.6
	Fe_3O_4 B	455	0.67	0.01	0.46	12.1
	Fe_5C_2 I	220	0.26	0.04	0.38	31.1
	Fe_5C_2 II	182	0.24	-0.01	0.36	26.2
	Fe_5C_2 III	100	0.16	-0.1	0.44	26.0
FTS run 168 h	Fe_3O_4 A	487	0.27	0.0	0.28	15.3
	Fe_3O_4 B	458	0.65	-0.01	0.50	43.2
	Fe_5C_2 I	218	0.27	0.04	0.90	23.9
	Fe_5C_2 II	180	0.19	0.09	0.28	5.1
	Fe_5C_2 III	100	0.18	0.11	0.68	12.5
FTS run 453 h	Fe_3O_4 A	488	0.28	0.01	0.25	32.2
	Fe_3O_4 B	459	0.65	0.0	0.32	67.8
	Fe_5C_2 I	----	----	----	----	----
	Fe_5C_2 II	----	----	----	----	----
	Fe_5C_2 III	----	----	----	----	----

CO conversion versus time on stream was plotted in Fig. 1 for unpromoted iron catalyst and Fig 2 for potassium promoted iron. After 24 hours of activation in CO, both catalysts exhibited high activity (over 80%), and the induction time to attain maximum conversion is very short. The activity of the catalyst slowly, but continuously, declined with increasing time-on-stream. The deactivation rate for the unpromoted iron is slower than for potassium promoted iron, as observed previously.

Mössbauer analysis results of samples (unpromoted iron) withdrawn from reactor are listed in Table 1. Immediately after CO activation, the catalyst composition was predominantly Hägg carbide (Fe_5C_2), and the Mössbauer spectrum of this sample contains very small magnetite

peaks. Fitting results revealed that 93.6% of iron phase is Hägg carbide. No metallic iron was detected. The spectrum of the sample removed after 23h of FT synthesis is more complicated; peaks of magnetite grows larger and overlap with the peaks of iron carbide. As indicated in Table 1, about 83.3% of spectra area was associated with Hägg carbide, and the area ratio of A to B patterns obtained for this phase was 0.76:2; still no metallic iron was found in the spectrum. After exposed to syngas for 168h, peaks of Hägg carbide became relatively lower and the area of magnetite contribute the largest part to the overall spectrum. The data show 58.5% of the iron exists in the form of magnetite and 41.5% Hägg carbide. The A to B site ratio is 0.71:2. The Mössbauer spectrum of sample removed after 453h of Fischer-Tropsch synthesis is simple since the amount of iron carbide is so low that it cannot be observed in the Mössbauer spectrum. The A to B site ratio is 0.95:2.

Discussion

The excellent agreement of catalytic activity with the percentage of iron carbide clearly shows that iron carbide is the active phase while the Fischer-Tropsch synthesis activity of magnetite is negligible.

Mössbauer studies of ultrafine iron catalyst by Huang et al., (4) suggested that after 24h of CO pretreatment, the catalyst was the carbide (ca. 4% iron oxide). With the increase of time on stream, reoxidation of iron carbide took place during the synthesis. After 100h of FT synthesis, no iron carbide can be observed in Mössbauer spectrum. Consistency of results on precipitated and ultrafine catalyst proved that our results are reliable and repeatable. The work described in this note also supports Huang et als. conclusion that CO pretreatment for 24h almost completely transform Fe_2O_3 to Hägg carbide even without the presence of potassium promoter.

Shroff et al (5) emphasized the importance of passivation of iron Fischer-Tropsch catalysts. They claimed that active phase of iron could get oxidized without sufficient attention to passivation. Mössbauer spectroscopy is an ex situ characterization technique. However, our results show that with appropriate methods to withdraw the sample from the reactor, remove wax and load into the sample holder, the iron active phase could be protected without oxidation. The fact that the initial sample withdrawn from the reactor is always found to be nearly all iron carbide eliminates sample contamination after withdrawal determining the sample compositin. Furthermore, sample contamination by oxidation by exposure to air should be random, and not to always show a gradual decline. The problem of only observing magnetite as the only detectable phase in the catalyst is most likely due to the sample handling method.

From our results, iron carbide is reoxidized to magnetite with increasing time-on-stream. Water and/or CO_2 are believed to be responsible for such oxidations (6). Rao et al. (7) studied the correlation of catalytic activity of iron catalyst promoted by potassium. They concluded that when a catalyst activation produces both an active catalyst and a high fraction of iron carbide, during the synthesis there will be a conversion of the carbide to the oxide with the attainment of a "pseudo-steady-state" composition. However, our result on precipitated unpromoted iron catalyst shows that oxidation of iron carbide takes place throughout the synthesis procedure. According to Amelse et al (8) and Bianchi et al (9), even at the low conversion rate, there is a strong interaction of water with iron surfaces. Actually, besides accelerating carburization, the alkali promoter is also believed to stabilize the carbidic phase (3,10). Therefore, the pseudo-steady-state is likely to happen only under the presence of alkali and other promoters which stabilize iron carbide from oxidation.

Magnetite has a unit cell composed of 32 close-packed oxygen atom in which cations occupy 8 tetrahedral (A) and 16 octahedral (B) sites (11). The theoretical value of the A to B ratio for the ideal spinel structure is 1:2. Generally, cation vacancies selectivity form on the B-sites; thereby producing a ratio greater than 1:2. A to B site ratios of our sample are 0.77:2 (after activation), 0.76:2 (after 23h FTS), 0.71:2 (after 168h FTS), and 0.95:2 (after 453h FTS). This means that A sites are not occupied by Fe ions. This appears to require that cation vacancies exist or carbon occupies the B-sites. If carbon occupies these sites, the fraction of carbon per "molecule" would be 0.23, 0.24, 0.29 and 0.05, respectively. Therefore, we concluded that magnetite phase contains carbon atoms on the A-sites, especially in the samples with the multiple phases.

The potassium promoted catalyst samples withdrawn from the reactor will be analyzed by Mossbauer spectroscopy and the data will be included in the next report.

References

4. J. P. Reymond, P. Meriaudeau and S. J. Teichner, *J. Catal*., **75** (1982) 39.

2. C. S. Kuivila, P. C. Stair, and J. B. Butt, *J. Catal*., **118** (1989) 299.

3. R. A. Dictor and A. T. Bell, *J. Catal*., **97** (1986) 121.

4. C. S. Huang, B. Ganguly, G. P. Huffman, F. E. Huggins and B. H. Davis, *Fuel Sci. Technol. Int*., **11** (1993) 1289.

5. M. D. Shroff and A. K. Datye, *Catal. Lett*., **37** (1996) 101.

6. J. F. Schulz, W. K. Hall, B. Seligman and R. B. Anderson, *J. Am. Chem. Soc*., **77** (1955) 213.

7. K. R. P. M. Rao, F. E. Huggins, G. P. Huffman, R. J. Gormley, R. J. O'Brien, B. H. Davis, *Energy & Fuel*, **10** (1996) 547.